Oscillator strengths for the beryllium isoelectronic sequence*

C. D. Lin† and W. R. Johnson‡
Center for Astrophysics, Harvard College Observatory and Smithsonian Astrophysical Observatory, Cambridge, Massachusetts 02138
(Received 19 October 1976)

Oscillator strengths for the outer shells of the beryllium isoelectronic sequence are obtained using the relativistic random phase approximation in which the relativistic effects are included nonperturbatively. The results agree well with other accurate calculations that have been carried out for low-Z elements. For high-Z elements, our results should be very reliable. Both length and velocity formulas are used to calculate the oscillator strengths. The velocity formula is very sensitive to the weak inner-shell coupling, whereas the length formula is not. Inner-shell excitation energies and oscillator strengths are examined and compared with the helium isoelectronic sequence to show the effect of outer-shell screening.

I. INTRODUCTION

Radiative transition rates of highly ionized atoms have many important applications in determining the density and temperature of the solor corona and of solar flares.[1] These data are also required in studying the energy loss in controlled thermonuclear plasmas.[2] Of these ions, the beryllium-like species are particularly important.

Accurate experimental determinations of transition rates are difficult.[3] Many theoretical methods have been designed to obtain accurate transition rates (or oscillator strengths) for the Be sequence. For low-Z ions, nonrelativistic theory is adequate. Large-scale configuration mixing has been employed[4] to obtain accurate wave functions for the initial and final states, from which oscillator strengths can be obtained. To achieve good convergence, variants of the configuration mixing methods have been used also. For example, a variational perturbation method using basis functions consisting of Hylleraas-type coordinates has been used recently.[5] The accuracy of the various methods depends upon the type and the number of configurations included and therefore is difficult to assess. Furthermore, these multiconfiguration calculations are very time consuming and not suitable for calculations along the entire isoelectronic sequence.

Other nonrelativistic methods which can be easily extended along the isoelectronic sequence are the Z-expansion method[6] and the random phase approximation.[7] This latter method is useful because of its computational simplicity and the accuracy with which it predicts oscillator strengths. However, all these nonrelativistic theories have inherent limitations. The relativistic effects which become more important with increasing Z are not included or are included only perturbatively.

Recently, several authors have developed configuration mixing methods[8,9] using relativistic wave functions to calculate oscillator strengths along the Be sequence up to very high Z. Since the number of configurations included in these relativistic calculations is small, the quality of the values obtained is uncertain and the length and velocity results show substantial disagreement.[9]

In recent papers,[10] we have presented a relativistic version of the random phase approximation (RPA) for the study of allowed and forbidden transition rates. Application of the method to the helium isoelectronic sequence indicates that it is very accurate in calculating the transition rates. The extension of the method to calculate Be-sequence oscillator strengths is straightforward.

For electric dipole transitions, both length and velocity formulas are used to evaluate the oscillator strengths. As in the nonrelativistic RPA, the two forms give identical results if the RPA equations are solved exactly.[11] In investigating the outer $2s$-shell excitation, the RPA equations contain small coupling terms involving the virtual excitations from the inner $1s$ shell. Despite the large energy separations between the two shells, we have found that the weak coupling terms are important in bringing the velocity result, which is changed substantially by the coupling, into agreement with the length result.

The relativistic RPA theory is summarized in Sec. II and the results of our calculations are discussed and compared with others in Sec. III. Inner-shell excitations of the $1s$ orbitals are examined and compared with the corresponding excitation in the He sequence to show the effect of outer-shell screening, in Sec. IV.

II. RELATIVISTIC RPA

Details of the relativistic method have been given by Johnson and Lin, Ref. 10 (henceforth referred to as I). Briefly, we start with a set of Dirac-Hartree-Fock (DHF) orbitals $u_i(\vec{r})$ for the occupied electrons. The perturbation $w_{i\pm}(\vec{r})$ introduced by the external field $A_+e^{-i\omega t}+A_-e^{+i\omega t}$ with frequency ω satisfies the relativistic equations

$$(h_0+V-\epsilon_i\mp\omega)w_{i\pm}=(A_\pm-V_\pm^{(1)})u_i\,. \tag{1}$$

For Be-like systems, $i=1, 2, 3, 4$. In Eq. (1), h_0 is the one-electron Dirac operator, V is the DHF potential, ϵ_i is the orbital energy, and $V_\pm^{(1)}$ represents the approximate correlation effect included in the RPA. The zeroth-order solution of (1) is the DHF equation for the excited orbital.

By separating the angular part from the radial part, Eq. (1) reduces to a set of coupled equations of the form

$$(\mathfrak{L}_i-\epsilon_i\mp\omega)\mathfrak{S}_i^\pm=O_i^\pm, \tag{2}$$

where

$$\mathfrak{S}_i^\pm\equiv\begin{pmatrix}S_i^\pm\\ T_i^\pm\end{pmatrix}$$

is the radial wave function. Equation (2) is a set of coupled integro-differential equations. Their explicit form is given in the Appendix.

For the $E1$ transition of the Be sequence, Eq. (2), explicitly given in the Appendix, defines a set of eight coupled radial differential equations. We solve these equations iteratively, treating the positive-frequency components separately from the negative-frequency components at each iteration. This reduces the number of coupled equations to four. The problem can be further simplified by recognizing that the couplings between the $1s$ and $2s$ shells are small and that these weak couplings can be treated perturbatively. Thus, the set of four coupled equation is reduced to two, representing the excitation from the $1s$ shell or the $2s$ shell, and may be treated independently in the first approximation. The decoupled equations are similar to the equations encountered in the helium problem of I and can be solved by analogous methods.

As in the nonrelativistic RPA, the oscillator strengths calculated using length and velocity formulas are identical provided that the RPA equations are solved *exactly*. Previous nonrelativistic RPA calculations either solve the RPA equations only approximately by expanding the solution over a finite basis set or use only the length formula.[7]

We have used both length and velocity formulas in the equivalent relativistic versions to calculate oscillator strengths in the relativistic equations. In I, these formulas served as a check on the accuracy of the numerical calculation and agreement to better than seven figures was achieved. Here we use the two forms to evaluate the oscillator strengths in the truncated and the full relativistic RPA calculations for the Be sequence. The results of these calculations are discussed below.

III. RESULTS

In Table I, we present the DHF, truncated, and full relativistic calculational results for the outer $2s$-shell excitations for several Be-like ions. The truncated relativistic RPA calculation is done by neglecting the coupling terms which represent the virtual excitations from the $1s^2$ shell. In the full relativistic RPA calculation this weak coupling has been included by a perturbation procedure. More details of the calculations are given in the Appendix.

The length and velocity results for low-Z elements differ substantially in the DHF calculation. In the truncated relativistic RPA calculation, these differences decrease but remain significant. By introducing the small couplings with the $1s^2$ shell in the full relativistic RPA, the length and velocity results then agree to better than four figures, the differences arising from the numerical accuracy of our iterative solution. The velocity results for the oscillator strengths are altered substantially by the inclusion of the weak coupling with the $1s$ shell, whereas the length results are modified only slightly. Hibbert *et al.*[4] found a similar behavior in configuration-interaction calculations in which the inclusion of inner-shell virtual excitations is important in bringing the two forms into harmony. The velocity form is sensitive to the wave functions at small distances where the coupling with $1s$ orbitals is significant. Similar conclusions hold for the transition to higher states and to the higher members of the Be sequence, though the effects are smaller. If the inner-shell couplings are completely neglected, the length form should be used.

We also list the results of our relativistic calculations for the intercombination oscillator strengths of the $2\,^1S_0-2\,^3P_1$ transitions in Table I. The difference in the length and velocity results are very large in the truncated relativistic RPA amounting to a factor of more than 2. By including the $1s^2$ coupling, the two results are brought into agreement, and the length results are only slightly changed. The agreement between length and velocity results in the full relativistic RPA calculations for the intercombination transition is not as good as for the allowed

TABLE I. Comparisons for Be-like ions of DHF, truncated, and full RRPA results for the oscillator strengths, obtained using length form (L) and velocity form (V) of the $E1$ transition operator.

Element			DHF	RRPA Truncated	RRPA Full	Others	
Be	$2\rightarrow 2$	L	2.05	1.388	1.379	1.3862,[e] 1.378,[c] 1.372[d]	
		V	1.06	1.441	1.378	1.3776,[e]	
	$2\rightarrow 3$	L	2.31(−4)	2.584(−2)	2.511(−2)	2.27(−2),[c] 2.25(−2)[d]	
		V	8.75(−5)	2.945(−2)	2.507(−2)		
	$2\rightarrow 4$	L	1.54(−3)	1.458(−3)	1.348(−3)	1.02(−3),[c] 2.0(−4)[d]	
		V	1.28(−3)	1.991(−3)	1.345(−3)		
C^{2+}	$2-2$	L	1.104	0.7604	0.7528	0.764,[e] 0.749,[c] 0.764[d]	
		V	0.684	0.8292	0.7523	0.762[e]	
	$2-3$	L	0.200	0.2135	0.2158	0.223,[c] 0.236[d]	
		V	0.193	0.2040	0.2159		
	$2-4$	L	6.97(−2)	7.746(−2)	7.834(−2)	7.75(−2),[c] 5.40(−2)[d]	
		V	6.76(−2)	7.722(−2)	7.835(−2)		
	$2-2'$	L	2.10(−7)	4.35(−8)	4.28(−8)	1.81(−7),[f] 1.27(−7),[h] 3.1(−7)[g]	1.87(−7)[a]
		V	2.64(−8)	1.01(−7)	4.66(−8)		
O^{4+}	$2\rightarrow 2$	L	0.728	0.504	0.4990	0.512,[e] 0.495,[c] 0.513[d]	
		V	0.498	0.562	0.4987	0.511,[e]	
	$2\rightarrow 3$	L	0.362	0.391	0.3936	0.400,[c] 0.406[d]	
		V	0.354	0.380	0.3936		
	$2\rightarrow 4$	L	0.111	0.120	0.1212	0.121,[c] 0.089[d]	
		V	0.109	0.117	0.1212		
	$2\rightarrow 2'$	L	1.98(−6)	5.62(−7)	5.55(−7)	1.62(−6),[f] 1.28(−6),[h] 2.4(−6)[g]	1.78(−6)[a]
		V	5.46(−7)	1.09(−6)	5.60(−7)		
Ar^{14+}	$2\rightarrow 2$	L	0.274	0.199	0.1976	0.209[b]	
		V	0.220	0.228	0.1976	0.240[b]	
	$2\rightarrow 3$	L	0.622	0.643	0.6445		
		V	0.617	0.636	0.6445		
	$2\rightarrow 4$	L	0.162	0.167	0.1673		
		V	0.161	0.162	0.1673		
	$2\rightarrow 2'$	L	3.24(−4)	1.36(−4)	1.355(−4)	2.2(−4)[b]	2.45(−4)[a]
		V	1.85(−4)	2.26(−4)	1.355(−4)	3.0(−4)[b]	
Mo^{38+}	$2\rightarrow 2$	L	0.164	0.140	0.1398	0.140[b]	
		V	0.150	0.151	0.1398	0.172[b]	
	$2\rightarrow 3$	L	0.503	0.510	0.5109		
		V	0.502	0.508	0.5109		
	$2\rightarrow 4$	L	0.127	0.128	0.1286		
		V	0.126	0.128	0.1286		
	$2\rightarrow 2'$	L	1.01(−2)	5.91(−3)	5.89(−3)	7.5(−3)[b]	6.78(−3)[a]
		V	7.49(−3)	8.08(−3)	5.89(−3)	1.27(−2)[b]	

[a]Semiempirical values obtained from the full RRPA results, corrected by using experimental or other more accurate theoretical energies. See text.
[b]Armstrong *et al.*, Ref. 9.
[c]Stewart, Ref. 7.
[d]Victor and Laughlin, Ref. 15.
[e]Moser *et al.*, Ref. 4.
[f]Laughlin and Victor, Ref. 12.
[g]Garstang, Ref. 14.
[h]Nussbaumer, Ref. 13.

dipole transition because of the greater numerical difficulty in obtaining the low-lying $^3P_1$ states. Indeed, our numerical scheme does not converge for the transition $2\,^3P_1 - 2\,^1S_0$ of Be. The lack of convergence is caused by the contribution from δ_k^- components to the final-state wave function which are very large, while our numerical method treats δ_k^- as small quantities.

The oscillator strengths for the allowed transitions are compared with other available calculations in Table I. For low-Z elements, a more detailed comparison has been presented recently

TABLE II. Intercombination line ($^1S_0$-$^3P_1$) oscillator strengths for the low-Z beryllium-like ions. Listed quantities are the experimental energies and the calculated energies of $(2s2p)^{1,3}P_1$ states, given in atomic units. The oscillator strengths under f_{RRPA} are obtained from the RRPA calculations. The column under f_{emp} gives the oscillator strengths obtained from f_{RRPA} by correcting for experimental energies, which is accomplished by multiplying by a factor

$$R=\frac{E_3(\text{exp})}{E_3(\text{RPA})}\times\frac{[E_1(\text{RPA})-E_3(\text{RPA})]^2}{[E_1(\text{exp})-E_3(\text{exp})]^2},$$

where E_1 and E_3 are the singlet and triplet energies from experiment or RRPA calculation.

Ion	Energy (exp) [a] Singlet	Triplet	Energy (RRPA) Singlet	Triplet	f_{RRPA}	f_{emp}	Others
C^{2+}	0.4663	0.2385	0.4282	0.1106	4.35(−8)	1.82(−7)	1.81(−7),[b] 3.1(−7),[c] 1.27(−7)[d]
N^{3+}	0.5955	0.3062	0.5438	0.1520	1.78(−7)	6.58(−7)	6.13(−7),[b] 9.1(−7),[c] 4.78(−7)[d]
O^{4+}	0.7235	0.3478	0.6577	0.2003	5.55(−7)	1.78(−6)	1.62(−6),[b] 2.4(−6),[c] 1.28(−6)[d]
F^{5+}	0.8513	0.4413	0.7711	0.2472	1.38(−6)	4.02(−6)	
Ne^{6+}	0.9794	0.5069	0.8848	0.2985	3.04(−6)	7.95(−6)	
Na^{7+}	1.1082	0.5777	0.9990	0.3436	5.81(−6)	1.49(−5)	
Mg^{8+}	1.2379	0.6468	1.1145	0.3981	1.07(−5)	2.55(−5)	
Al^{9+}	1.3687	0.7133	1.2316	0.4432	1.77(−5)	4.12(−5)	
Si^{10+}	1.5009	0.7817	1.3508	0.5000	2.91(−5)	6.37(−5)	

[a] All energies are from Moore, Ref. 16, except Ne^{6+} which are from Wiese *et al.*, Ref. 17.
[b] Laughlin and Victor, Ref. 12.
[c] Garstang and Shamey, Ref. 14.
[d] Nussbaumer, Ref. 13.

by Moser *et al.*[4] We list the values which we believe are the most accurate. The results demonstrate the reliability of the relativistic RPA calculations. The good agreement at low Z suggests that relativistic RPA results for higher Z where comparison data are not available are reliable. Our values indicate that the length results of Armstrong *et al.*[9] at higher Z, are superior to their velocity results.

For the intercombination line $2\,^3P_1 \rightarrow 2\,^1S_0$, our full relativistic RPA results disagree with the model potential calculations of Laughlin and Victor,[12] of Nussbaumer[13] and the semiempirical results of Garstang and Shamey.[14] This disagreement arises from the low accuracy of the energies calculated in the relativistic RPA. We can correct this error by following the approach used in I; Since we know that the intercombination transition matrix element is inversely proportional to the energy difference between the singlet and triplet states, a semiempirical correction to the oscillator strength is obtained by multiplying the full relativistic RPA values by R^2, where R is the ratio of the calculated to the experimental energy

TABLE III. Truncated RRPA values of the allowed and forbidden oscillator strengths in the Be sequence. $(2\rightarrow n)$ denotes allowed transitions to states with principal quantum number n and $(2\rightarrow n')$ designates forbidden transitions. Comparison values are presented under the headings f_L and (f_V).

	$2\rightarrow 2$	$f_L(f_V)$ [a]	$2\rightarrow 3$	$(2\rightarrow 3')$	$2\rightarrow 4$	$(2\rightarrow 4')$
Ne^{6+}	0.378	0.397(0.401)	0.493		0.143	
Mg^{8+}	0.304		0.558		0.154	
Al^{9+}	0.278		0.581		0.159	
Si^{10+}	0.256		0.601		0.162	
S^{12+}	0.223		0.628		0.166	
Ca^{16+}	0.181		0.648	(0.031)	0.166	(0.012)
Ti^{18+}	0.167		0.644		0.163	
V^{19+}	0.162		0.639	(0.058)	0.161	(0.018)
Fe^{22+}	0.150	0.156(0.190)	0.620		0.154	
Ni^{24+}	0.144		0.604	(0.113)	0.150	(0.032)
Cu^{25+}	0.142		0.596		0.148	
Kr^{32+}	0.136	0.137(0.171)	0.545	(0.181)	0.136	(0.047)
Mo^{38+}	0.140		0.510		0.128	
Xe^{50+}	0.173	0.168(0.193)	0.453	(0.243)	0.117	(0.059)

[a] Armstrong *et al.*, Ref. 9.

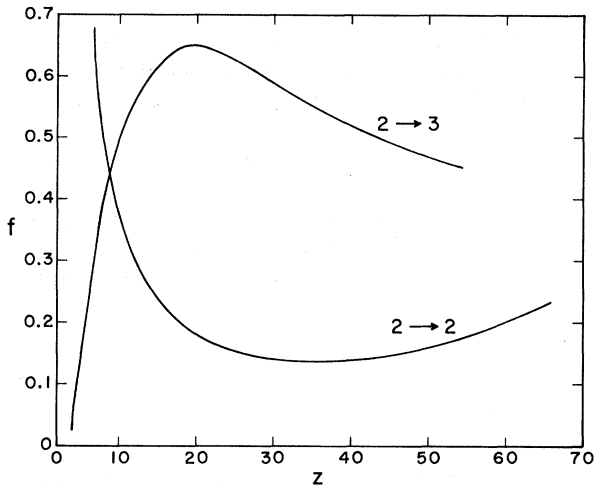

FIG. 1. Oscillator strengths for the transition $2\,^1S_0 \rightarrow 2\,^1P_1$ and $2\,^1S_0 \rightarrow 3\,^1P_1$ are given as functions of nuclear charge Z.

difference between the singlet and triplet states. In the beryllium sequence, the excitation energy is also poorly predicted. By using the experimental energies instead of the relativistic RPA values, we obtain the modified oscillator strengths, shown under the column "semiempirical." These values agree reasonably well with the model potential values of Laughlin and Victor[12] for C^{2+} and O^{4+}. For higher-Z elements, our semiempirical values agree with the length results of Armstrong *et al.*[9] Therefore, for practical purposes, we believe our semiempirical values are adequate for low-Z elements. For higher-Z elements (say $Z \geq 18$), the methods of Armstrong *et al.*[9] may provide adequate accuracy for this intercombination transition. Table II gives the semiempirical rates for the transition $2\,^3P_1 \rightarrow 2\,^1S_0$ for several elements not listed in Table I. For higher-Z elements, the rates can be obtained by interpolating between the length results of Armstrong *et al.*[9]

TABLE IV. Excitation energy difference between the helium sequence and the beryllium sequence for the transition $(1s^2)\,^1S_0 \rightarrow (1s2p)^{1,3}P_1$.

Element	Z	$\Delta E(^1P_1)$ [a]	$\Delta E(^3P_1)$ [a]
Be	4	0.2186	0.1917
C	6	0.4472	0.4131
O	8	0.6625	0.6254
Ne	10	0.8745	0.8356
Mg	12	1.0861	1.0452
Si	14	1.2976	1.2552
S	16	1.5102	1.4659
Ar	18	1.7157	1.6739
Ca	20	1.9401	1.8902
Ti	22	2.1583	2.1042
Fe	26	2.6032	2.5362
Cu	29	2.9458	2.8644

[a] Energy differences are given in atomic units. The value is the excitation energy of He-like ions subtracted from the excitation energy of Be-like ions. To obtain absolute excitation energy for Be-like ions, subtract the value given above from the corresponding excitation energy of He-like ions given in Ref. 10.

In Table III, we present the results of truncated relativistic RPA calculations using the length formula, they are probably accurate to within 5% of the full relativistic RPA. Transitions to the $2\,^1P_1$, $3\,^1P_1$, and $4\,^1P_1$ states are presented. In Table III we give the "forbidden transition" to the $3\,^3P_1$ and $4\,^3P_1$ states for several elements also, for higher-Z elements they are not small compared to the allowed transitions. We compare our results for the resonance transition with those of Armstrong *et al.*[9] For large-Z elements, their length results are almost identical to our relativistic RPA results. The distribution of oscillator strengths along the isoelectronic sequence is illustrated in Fig. 1 which shows the oscillator strengths of $2\,^1S_0 \rightarrow 2\,^1P_1$ and $2\,^1S_0 \rightarrow 3\,^1P_1$ against Z.

IV. INNER-SHELL TRANSITIONS

We have also investigated the inner $1s$ shell transitions in the Be sequence. The transition energies are more reliable than the corresponding transitions from the outer $2s$ shell. By comparing the calculated transition energies with the corresponding transitions in the He sequence, we can study the effect of outer-shell screening. These inner-shell calculations do not include outer-shell interactions, and therefore represent unshifted autoionization energies.

In the Be-sequence calculation, we did not include the Breit interaction terms. Thus, we compare the values calculated here with the He-se-

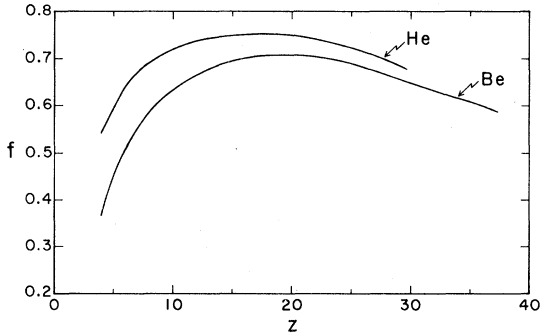

FIG. 2. Comparison of the $(1s^2)\,^1S_0 \rightarrow (1s2p)\,^1P_1$ inner-shell excitation oscillator strength in the Be sequence and the corresponding $^1S_0 \rightarrow {}^1P_1$ strength in the He sequence.

quence values, also without the Breit terms. Since the Breit terms are very complicated and not modified much by the outer-shell screening, the change in energies due to the Breit terms should be approximately equal in the two cases for the transition $1s^2 \rightarrow 2^{1,3}P_1$. In Table IV, we present the energy difference between the He sequence and the Be sequence. To obtain more accurate energies for the inner-shell transitions in the Be sequence, one can substract the values in Table IV from the corresponding He-sequence values.[18]

Comparisons of the oscillator strengths for the transition $(1s^2)^1S_0 \rightarrow (1s2p)^1P_1$ between He and Be sequence are shown in Fig. 2. For each Z, the Be-like ion oscillator strengths are less than those of the He-like ions. The difference cannot be explained by the excitation energy difference only. The transition matrix elements are also changed by the outer-shell screening.

V. DISCUSSION

In this paper, we have shown that relativistic RPA can be easily applied to many electrons system along an isoelectronic sequence. The oscillator strengths obtained for the allowed transitions are very accurate. We can study the highly ionized systems where experimental data are very scarce. For the intercombination line, our semiempirical values are probably accurate enough for most practical purposes. In Table II, we have supplied the rates for several elements which have not been investigated previously.

The relativistic RPA calculations done here for the Be sequence are not as complete as our previous calculations for the He sequence because we have neglected the Breit interaction terms entirely. Our experience in He sequence indicates that the Breit interactions can change the final oscillator strengths up to 15% at high Z. In the outer-shell $2s^2 \rightarrow (2s2p)^{1,3}P_1$ transitions of Be isoelectronic sequence, the effect is probably smaller because the excitation energy is small.

Our results indicate that the relativistic RPA is an efficient and effective tool for investigating radiative transitions in highly ionized atoms. Extensions of the method to other many-electron systems are now underway.

APPENDIX

The DHF orbitals $u_i(\vec{r})$ introduced in the text and used in Eq. (1) can be decomposed in a spherical basis as

$$u_i(\vec{r}) = \frac{1}{r}\begin{pmatrix} iG_i(r)\Omega_{\kappa_i m_i}(\hat{r}) \\ F_i(r)\Omega_{-\kappa_i m_i}(\hat{r}) \end{pmatrix}, \tag{A1}$$

where $\Omega_{\kappa_i m_i}(\hat{r})$ are spherical spinors (the subscripts κ_i and m_i being the usual relativistic electron angular momentum indices) and where $G_i(r)$ and $F_i(r)$ are large and small component radial functions. In a similar way the perturbed orbitals $w_i^{\pm}(r)$ can be expressed in terms of angular momentum states which in turn can be decomposed in a spherical basis. Suppose $w^{\pm}_{\kappa_j m_j}(r)$ represents that part of a perturbed orbital with angular momentum κ_j, m_j; then in parallel with (A1) we have

$$w^{\pm}_{\kappa_j m_j}(\vec{r}) = \frac{1}{r}\begin{pmatrix} iS_j^{\pm}(r)\Omega_{\kappa_j m_j}(\hat{r}) \\ T_j^{\pm}(r)\Omega_{-\kappa_j m_j}(\hat{r}) \end{pmatrix}, \tag{A2}$$

where $S_j^{\pm}(r)$ and $T_j^{\pm}(r)$ are large component and small component radial functions. After factoring the angular parts of the RPA equations (1), we are left with a set of coupled radial equations. For simplicity we collect together the unperturbed radial functions $G_{1s}(r)$ and $F_{1s}(r)$ in a single two-component radial function $\mathfrak{F}_{1s}(r)$:

$$\mathfrak{F}_{1s}(r) = \begin{pmatrix} G_{1s}(r) \\ F_{1s}(r) \end{pmatrix}. \tag{A3}$$

We define the two-component function $\mathfrak{F}_{2s}(r)$ in terms of $G_{2s}(r)$ and $F_{2s}(r)$ by a similar expression. The two-component perturbed orbital radial functions are denoted by $\mathfrak{S}_j^{\pm}(r)$ and Eq. (3) of the text gives $\mathfrak{S}_i^{\pm}(r)$ in terms of large and small component radial functions $S_i^{\pm}(r)$ and $T_i^{\pm}(r)$. For an electric dipole perturbation we must consider excitations leading to a $J=1$, negative parity final state. There are four possible excited orbitals of definite angular momentum to consider, which we label by subscripts a, b, c, and d. The subscripts a and b refer to excitations $1s \rightarrow p_{1/2}$ and $1s \rightarrow p_{3/2}$, while c and d refer to excitations $2s \rightarrow p_{1/2}$ and $2s \rightarrow p_{3/2}$; thus a and b are core excitations and c and d are valence excitations.

The radial RPA equations which govern the radial excitations $\mathfrak{S}_i^{\pm}(r)$ are written out in Eq. (2) of the text as

$$(\mathfrak{L}_i - \epsilon_i \mp \omega)\mathfrak{S}_i^{\pm} = O_i^{\pm}, \tag{2}$$

where $\epsilon_a = \epsilon_b = \epsilon_{1s}$, $\epsilon_c = \epsilon_d = \epsilon_{2s}$, and where the linear differential operator $\mathfrak{L}_i$ is given by

$$\mathfrak{L}_i(r) = \begin{bmatrix} m + V_i(r) & \dfrac{d}{dr} - \dfrac{\kappa_i}{r} \\ -\dfrac{d}{dr} - \dfrac{\kappa_i}{r} & m - V_i(r) \end{bmatrix}. \tag{A4}$$

The potential energy $V_i(r)$ is the Hartree-Fock ion potential, viz.,

$$V_a = V_b = -\frac{Z}{r} + \frac{2Y_0(2s,r)}{r} + \frac{Y_0(1s,r)}{r},$$
$$V_c = V_d = -\frac{Z}{r} + \frac{Y_0(2s,r)}{r} + \frac{2Y_0(1s,r)}{r}. \quad \text{(A5)}$$

The inhomogeneous coupling terms $O_i^{\pm}$ in Eqs. (2) satisfy the symmetry requirement that a complete interchange of orbitals $a \rightleftharpoons c$, $b \rightleftharpoons d$, $1s \rightleftharpoons 2s$ transforms $O_{a,b}^{\pm}(r) \rightleftharpoons O_{c,d}^{\pm}(r)$. It is therefore sufficient to write out $O_{c,d}^{\pm}(r)$ only since we can use the interchange symmetry to determine $O_{a,b}^{\pm}(r)$. We write

$$O_{c,d}^{\pm}(r) = A_{c,d}^{\pm}(r)\mathfrak{F}_{2s} + B_{c,d}^{\pm}(r)\mathfrak{F}_{2s} + C_{c,d}^{\pm}(r)\mathfrak{F}_{1s} + (1/r)Y_0(1s,2s,r)\mathfrak{S}_{a,b}^{\pm}(r). \quad \text{(A6)}$$

In Eq. (A6) we have

$$A_c^{\pm} = (1/r)[\tfrac{1}{9}Y_1(2s,c^{\pm},r) - \tfrac{4}{9}Y_1(2s,d^{\pm},r) - \tfrac{1}{3}Y_1(2s,c^{\mp},r)], \quad \text{(A7)}$$

$$A_d^{\pm} = (1/r)[-\tfrac{2}{9}Y_1(2s,c^{\pm},r) - \tfrac{1}{9}Y_1(2s,d^{\pm},r) - \tfrac{1}{3}Y_1(2s,d^{\mp},r)], \quad \text{(A8)}$$

$$B_c^{\pm} = B_d^{\pm} = (1/r)[-\tfrac{2}{9}Y_1(1s,a^{\pm},r) - \tfrac{2}{9}Y_1(1s,a^{\mp},r) - \tfrac{4}{9}Y_1(1s,b^{\pm},r) - \tfrac{4}{9}Y_1(1s,b^{\mp},r)], \quad \text{(A9)}$$

$$C_c^{\pm} = (1/r)[\tfrac{1}{3}Y_1(1s,c^{\pm},r) - \tfrac{1}{9}Y_1(2s,a^{\mp},r) + \tfrac{4}{9}Y_1(2s,b^{\mp},r)], \quad \text{(A10)}$$

$$C_d^{\pm} = (1/r)[\tfrac{1}{3}Y_1(1s,d^{\pm},r) + \tfrac{2}{9}Y_1(2s,a^{\mp},r) + \tfrac{1}{9}Y_1(2s,b^{\mp},r)]. \quad \text{(A11)}$$

In the equations above we have designated the Hartree screening functions by Y_k; these functions are defined by

$$Y_1(j,i^{\pm},r) = \frac{1}{r}\int_0^r dr\, r(G_j S_i^{\pm} + F_j T_i^{\pm}) + r^2\int_r^{\infty}\frac{dr}{r^2}(G_j S_i^{\pm} + F_j T_i^{\pm}) \quad \text{(A12)}$$

and

$$Y_0(j,l,r) = \int_0^r dr\,(G_j G_l + F_j F_l) + r\int_r^{\infty}\frac{dr}{r}(G_j G_l + F_j F_l). \quad \text{(A13)}$$

The functions $Y_0(i,r)$ occurring in Eq. (A5) are given by

$$Y_0(i,r) = Y_0(i,i,r). \quad \text{(A14)}$$

Our procedures for solving Eq. (2) parallel that outlined in I for the simpler equations of the He case.

---

*W. R. J. supported in part by NSF Grant No. GP-42738 and C. D. L. supported in part by ERDA Contract No. E(11-1)-2887.

†Permanent address: Department of Physics, University of Notre Dame, Notre Dame, Ind. 46556.

‡Permanent address: Department of Physics, Kansas State University, Manhattan, Kans. 66506.

[1]A. H. Gabriel and C. Jordan, *Case Studies in Atomic Collision Physics II* (North-Holland, Amsterdam, 1972), p. 211.

[2]E. Hinnov, Princeton University Report No. MATT-1022, 1974 (unpublished).

[3]I. Martinson, A. Gaupp, and L. J. Curtis, J. Phys. B 7, L463 (1974).

[4]C. M. Moser, R. K. Nesbet, and M. N. Gupta, Phys. Rev. A 13, 17 (1976); C. A. Nicolaides, D. R. Beck, and O. Sinanoğlu, J. Phys. B 6, 62 (1973); A. Hibbert, J. Phys. B 7, 1417 (1974); P. G. Burke, A. Hibbert, and W. D. Robb, J. Phys. B 5, 37 (1972).

[5]J. S. Sims and R. C. Whitten, Phys. Rev. A 8, 2220 (1973).

[6]D. K. Watson and S. V. Oneil, Phys. Rev. A 12, 729 (1975).

[7]R. F. Stewart, J. Phys. B 8, 1 (1975).

[8]Y. K. Kim and J. P. Desclaux, Phys. Rev. Lett. 36, 139 (1976).

[9]L. Armstrong, Jr., W. R. Fielder, and D. L. Lin, Phys. Rev. A 14 (1976).

[10]W. R. Johnson and C. D. Lin, Phys. Rev. A 14, 565 (1976), this paper is called I. W. R. Johnson, C. D. Lin, and A. Dalgarno, J. Phys. B 9, L303 (1976); C. D. Lin, W. R. Johnson, and A. Dalgarno, Phys. Rev. A 15, 154 (1977).

[11]See M. Ya Amusia and N. A. Cherephov, Case Stud. At. Phys. 5, 47 (1975); D. L. Yeager and V. McKoy, J. Chem. Phys. 61, 755 (1974).

[12]C. Laughlin and G. A. Victor (private communication).

[13]H. Nussbaumer, Astron. Astrophys. 16, 77 (1972).

[14]R. H. Garstang and L. J. Shamey, Astrophys. J. 148, 665 (1967).

[15]G. A. Victor and C. Laughlin, Nucl. Instrum. Meth. 110, 189 (1973).

[16]C. E. Moore, *Atomic Energy Levels*, NBS Circ. No. 467 (U.S. GPO, Washington, D.C., 1949), Vol. I.

[17]W. L. Wiese, M. W. Smith and B. M. Glennon, *Atomic Transition Probabilities* (U.S. GPO, Washington, D. C., 1966), Vol. I.

[18]C. D. Lin and W. R. Johnson, At. Data (to be published).